MOLECULAR AND CELLULAR BIOLOGY, Apr. 1988, p. 1684–1696
0270-7306/88/041684-13$02.00/0

Vol. 8, No. 4

Mapping Functional Regions of Transcription Factor TFIIIA

KENT E. VRANA,[1]† MAIR E. A. CHURCHILL,[2] THOMAS D. TULLIUS,[2] AND DONALD D. BROWN[1]*

Department of Embryology, Carnegie Institution of Washington, 115 West University Parkway, Baltimore, Maryland 21210,[1] and Department of Chemistry, The Johns Hopkins University, Baltimore, Maryland 21218[2]

Received 26 October 1987/Accepted 15 January 1988

Functional deletion mutants of the *trans*-acting factor TFIIIA, truncated at both ends of the molecule, have been expressed by in vitro transcription of a cDNA clone and subsequent cell-free translation of the synthetic mRNAs. A region of TFIIIA 19 amino acids or less, near the carboxyl terminus, is critical for maximal transcription and lies outside the DNA-binding domain. The elongated protein can be aligned over the internal control region (ICR) of the *Xenopus* 5S RNA gene with its carboxyl terminus oriented toward the 5′ end of the gene and its amino terminus oriented toward the 3′ end of the gene. The nine "zinc fingers" and the linkers that separate them comprise 80% of the protein mass and correspond to the DNA-binding domain of TFIIIA. The zinc fingers near the amino terminus of the protein contribute more to the overall binding energy of the protein to the ICR than do the zinc fingers near the carboxyl end. The most striking feature of TFIIIA is its modular structure. This is demonstrated by the fact that each zinc finger binds to just one of three short nucleotide sequences within the ICR.

TFIIIA is a positive, *trans*-acting factor required for transcription of 5S RNA genes in *Xenopus laevis*. It was first purified from *Xenopus* ovaries and shown to be a protein of about 38,500 daltons (12). One molecule of TFIIIA binds to the internal control region (ICR) of a 5S RNA gene (31, 42) nucleating the formation of a transcription complex (6) that involves at least two other factors (22, 41). This complex is required for RNA polymerase III to initiate transcription accurately at the start site of the 5S RNA gene.

Analysis of TFIIIA proteolytic fragments suggests that the protein is composed of a transcription and a DNA-binding domain (42). The carboxyl terminus of TFIIIA (43) is required for the full transcriptional activity of the factor but not for the sequence-specific binding of the protein to the ICR (42). These data suggested that the binding domain of the protein can be aligned over the ICR with its carboxyl terminus toward the 5′ end and its amino terminus toward the 3′ end of the ICR. This picture of an asymmetric, elongated protein molecule is reinforced by its physical properties in solution (3). Deletion mutants of the ICR show clearly that binding of the protein is not uniform over the ICR since binding to the 3′ end of the ICR is required for binding at the 5′ end but not the reverse (39). Protection of G residues from methylation by TFIIIA is strongest at the 3′ end of the ICR and weakest at the 5′ end (13).

The gene for TFIIIA has been isolated from cDNA libraries prepared from *Xenopus* ovaries (16, 43). The protein sequence predicted from the cDNA sequence is composed predominantly of nine imperfect, tandemly repeated regions, each approximately 30 amino acids in length (10, 30). The conserved sequence includes pairs of cysteines and histidines, amino acids known to bind metal ions in proteins. It had been shown previously that TFIIIA contains zinc (19). Each adjacent repeated polypeptide and its associated zinc atom (called "zinc finger") has been postulated to interact with a repeated sequence element within the ICR (34). This putative DNA repeat is characterized by one or more G residues (on the noncoding strand), repeated on average every 5.5 base pairs along the ICR.

In these experiments, we further characterized this DNA-protein interaction, using deletion mutants of TFIIIA prepared by a recently described method (20). Messenger RNA was transcribed in vitro by a bacteriophage polymerase from various cDNA constructs. The resultant mRNA was translated in a wheat germ extract in vitro, and the newly synthesized protein was then tested for its ability to bind to the 5S RNA gene and to support 5S RNA transcription. Binding was assayed both by DNase I footprinting (14) and by a new chemical method that makes use of hydroxyl radicals to cleave the DNA backbone (45, 46). The results of these experiments give a detailed projection of specific regions of the protein onto their cognate sequences within the ICR and support the modular nature of TFIIIA predicted by the zinc finger model.

MATERIALS AND METHODS

In vitro transcription of the cDNA for TFIIIA. The full-length TFIIIA cDNA used in these experiments was isolated originally from a library prepared from *X. laevis* oocytes and constructed in λ gt10 by D. Melton (16). The *Eco*RI insert was subcloned into the *Eco*RI site of pSP65 (Fig. 1). Transcription from the SP6 promoter of this construct generates mRNA for the TFIIIA molecule. Transcription was conducted, in a volume of 200 μl, as previously described by Melton et al. (29). To produce translation-competent (capped) mRNA molecules, we included the capped precursor ^{7}mGpppGm (P-L Biochemicals, Inc.) at a concentration of 500 μM (D. Melton, personal communication).

In vitro translation of synthetic messenger RNA. The synthetic RNA generated by SP6 transcription was translated in a cell-free wheat germ extract, using an amino acid mixture lacking cysteine (Bethesda Research Laboratories). The synthesized protein was labeled by including [^{35}S]cysteine (250 mM; 1.5 Ci/mol). Translated proteins were electropho-

* Corresponding author.
† Present address: Department of Biochemistry, West Virginia University School of Medicine, Morgantown, WV 26506.

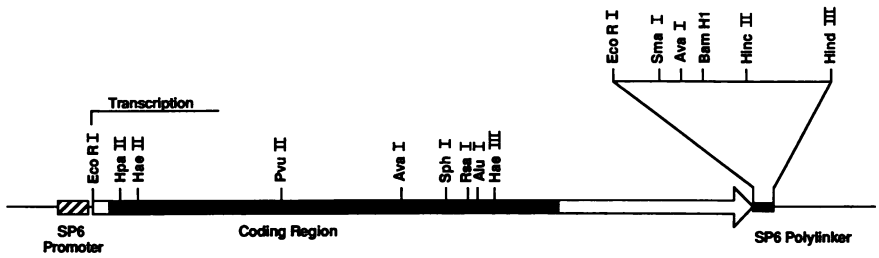

FIG. 1. Restriction endonuclease map for pSPTF15. This map represents the original construct (in pSP65) from which the TFIIIA was synthesized and from which deletion mutants were constructed.

resed in a 15% polyacrylamide gel (acrylamide-bisacryl, amide, 30:0.3) using the conditions of Ryrie and Galagher (36) with a 7.5% stacking gel. Following electrophoresis, the gel was soaked for 30 min in 1 M sodium salicylate, dried onto Whatman 3MM paper, and autoradiographed. Molecular weight determinations were made using ^{14}C-methylated protein molecular weight markers (Bethesda Research Laboratories). The yield of TFIIIA for each mutant was determined by excising the band of interest following autoradiography and determining the incorporation of radioactivity by liquid scintillation spectrometry. Molar yields of the various mutants were corrected for the number of cysteines present in each molecule.

Construction of the deletion mutants of TFIIIA. The carboxyl-terminal mutants were constructed in three ways. CΔ89, CΔ212, and CΔ121 were synthesized from pSPTF15 following digestion of the parent plasmids with *Sph*I, *Pvu*II, and *Ava*I, respectively (Fig. 1). The last two DNA molecules were transcribed directly following purification of the plasmid and digestion with the respective enzymes. The *Sph*I digestion generates a 3′ overhang, however, which is incompatible with accurate initiation of SP6 transcription. Therefore, the ends were repaired with T4 DNA polymerase and deoxynucleotides prior to transcription.

CΔ31, CΔ135, CΔ170, and CΔ185 were generated from an exonuclease III-S1 nuclease deletion series constructed as described by Sakonju et al. (37). Briefly, pSPTF15 (Fig. 1) was digested with *Bam*HI and then digested for various periods of time with exonuclease III. After the resulting single strands were removed with S1 nuclease, the ends were repaired with T4 DNA polymerase and the inserts were excised with *Eco*RI. This mixture of truncated molecules was then ligated into *Eco*RI-*Sma*I-digested pSP65 treated with alkaline phosphatase, and the DNA was transformed into the DH-1 strain of *Escherichia coli*. Colonies harboring TFIIIA sequences were identified by hybridization (18) and screened for inserts of the desired size. The final determination of the endpoints was made by chemical sequencing (2). Transcription of these constructs was performed after linearizing the plasmids with *Bam*HI (the *Sma*I restriction site is destroyed by the cloning procedure).

CΔ50, CΔ62, and CΔ70 were constructed using, respectively, *Ava*I-*Hae*III, *Ava*I-*Alu*I, and *Ava*I-*Rsa*I fragments isolated from pSPTF15. The appropriate gel-purified fragments were cloned into *Ava*I-*Hin*cII-digested pSPT15 because there is an *Ava*I site present in the polylinker of SP65 distal to the *Sma*I site used previously. These constructs were linearized with *Hin*dIII prior to their use in a transcription reaction.

The amino-terminal deletion series was generated by using two methods. NΔ6 and NΔ17 were synthesized by digesting pSPTF15 with *Hpa*II and *Hae*II, respectively. The initiator methionine for each construct was then added by ligating the NΔ6 (i) and NΔ17 (ii) adapters (synthesized on an Applied Biosystems 380A oligonucleotide synthesizer), shown below, onto each digested plasmid molecule:

Met

AATTC AAGGA GAGA TGC (i)

----GTTCCT CTCT ACGGC

Met

AATTCCAG GAGAGA TGGCCGAC TGCGGCGC (ii)

----GGTCC TCTCTA CCGGCT GACGC----

Following ligation, the desired fragments were excised from the plasmid with *Eco*RI and then cloned into the *Eco*RI site of pSP65. Recombinants bearing TFIIIA-coding sequences were identified by hybridization, and the orientation was determined by restriction mapping. The sequence 5′ to the initiator ATG represents the 5′ untranslated sequence in the pSPTF15 clone and was chosen to maintain the integrity of the initiation site as much as possible.

The remaining two deletion mutants (NΔ55 and NΔ62) were constructed from an exonuclease III-S1 nuclease library generated as described for the carboxyl deletion series above but starting with a clone (pSPTF14) in the opposite orientation so that the 5′ end of the gene was nearest the *Bam*HI site. After the ends of the deletion series were repaired with T4 DNA polymerase, the adapter shown below was ligated onto the ends of the deletions:

Met

AATTCAAGGAGAGATG

----GTTCCTCTCTAC

Again the inserts were excised with *Eco*RI, and the molecules were cloned into *Eco*RI-digested pSP65. Screening was as above except that here we expected only one out of every three constructs to be in the correct reading frame. We therefore prepared RNA from seven clones that had been found to have inserts of the correct size and screened the RNA molecules, by in vitro translation, for the correct reading frames. Four positive clones were identified. The endpoints of two of these were confirmed by sequencing. Transcription of all of the amino terminal mutants was conducted with plasmids linearized with *Bam*HI.

Immunologic depletion of oocyte nuclear extract and transcription reconstitution reactions. Oocyte nuclear extract

(100 μl; 4) was incubated for 30 min on ice with 40 μl of purified immunoglobulin G antibody (3 mg/ml) directed against TFIIIA. At this point, the immunoglobulin G-TFIIIA complex was adsorbed with 60 μl of protein A-Sepharose (Sigma Chemical Co.; 1:1 [vol/vol] in phosphate-buffered saline) for 30 min on ice with frequent mixing by hand. The Sepharose complex was then centrifuged in an Eppendorf Microfuge at 4°C for 1 min, and the supernatant was used for transcription reconstitution experiments.

The transcription reconstitution experiments with immunologically depleted oocyte nuclear extract were conducted as previously described (42) with the following modifications. The reaction was conducted with 4.5 μl of depleted oocyte nuclear extract in a final volume of 15 μl. The tRNA (pXltmet) and 5S RNA (pXbs201) plasmid templates were present at 1 μg/ml with a final DNA concentration of 10 μg/ml made up with pSP65. This concentration of pXbs201 is 7 fmol/15 μl. Each reaction contained 10 U of human placental ribonuclease inhibitor (RNasin; Amersham Corp.). Synthetic TFIIIA or a mutant was added to the reaction at a concentration of 35 fmol/15 μl (fivefold molar excess of protein over 5S RNA gene) in a total volume of 5.25 μl of wheat germ translation extract. The volumes were corrected, as necessary, with translation extract that had not been programmed with mRNA.

DNase I protection assays. DNase I footprinting was conducted as described by Smith et al. (42), using the *Xenopus borealis* somatic 5S RNA gene called pXbs201. Synthetic TFIIIA or mutant factor (present in a wheat germ translation mixture) was added to a 40-μl reaction mixture. The factor concentration was held constant. The total wheat germ extract volume was normally 7 μl, with the difference in volume between preparations made up with a translation reaction prepared in the absence of mRNA. As with the transcription reactions, TFIIIA or mutant protein was added at a fivefold molar excess over DNA.

Preparation of DNA for hydroxyl radical footprinting. Hydroxyl radical protection experiments require DNA templates of very high quality. For this reason, pXbs201 was isolated and purified by a modified version of a cleared lysate procedure that produces a minimal amount of nicked DNA (45, 46). The plasmid was linearized with either *Hin*dIII or *Bam*HI and end labeled by filling in the 5′ overhang with three α-^{32}P-labeled deoxynucleotide triphosphates (3,000 to 7,000 Ci/mmol; Amersham Corp.) and one dideoxynucleotide triphosphate (P-L Biochemicals), using the Klenow fragment of DNA polymerase I (Bethesda Research Laboratories). A second digestion with *Bam*HI or *Hin*dIII (depending on the labeled end) generated a 249-base-pair fragment containing the 5S RNA gene and surrounding sequences. The fragment was isolated by electrophoresis on an 8% polyacrylamide gel and purified by the Maxam and Gilbert (26) crush-and-soak procedure. Two phenol extractions, followed by two ether extractions, were necessary to remove gel material that interferes with TFIIIA binding. Omission of these steps or substitution of the phenol by phenol-chloroform-isoamyl alcohol resulted in poor protein binding. A fraction of the purified DNA was analyzed for radioactive incorporation to determine the yield (typically, 60 to 80% of theoretical yield) and to quantitate the concentration of DNA.

Hydroxyl radical footprinting. Hydroxyl radical footprinting experiments were carried out at a TFIIIA-to-DNA ratio of 10 mol of factor per mol of DNA fragment for all of the mutants except CΔ212, which required a ratio of 40 to 1. A wheat germ extract containing in vitro-synthesized TFIIIA or mutant proteins was diluted to an appropriate concentration with translation extract containing no mRNA. The DNA solution (14 μl) contained 4.0 fmol of end-labeled DNA and 0.4 μg of plasmid carrier DNA (pBR322) in 1× TFIIIA-binding buffer (20 mM sodium HEPES [*N*-2-hydroxyethylpiperazine-*N*′-2-ethanesulfonic acid] [pH 7.5], 70 mM NH_4Cl, 7 mM $MgCl_2$, 10 μM $ZnCl_2$, and 0.02% Nonidet P-40). Since glycerol is an effective scavenging agent for hydroxyl radical, it was omitted (46) from the normal TFIIIA-binding buffer (42). The DNA solution was added to 7 μl of wheat germ extract containing TFIIIA or mutant protein, mixed gently, and allowed to stand on ice for 30 min. Each extract-DNA mixture was warmed to room temperature (22°C) over a period of 2 min and allowed to react with hydroxyl radical. The cleavage reagent (hydroxyl radical-generating system) consisted of 1.25 μl each of iron(II) EDTA solution [1 mM iron(II), 2 mM EDTA], 0.06% H_2O_2, and 20 mM sodium ascorbate. The three solutions were placed on the wall of the reaction vial above the DNA-extract mixture, mixed together, and then mixed with the extract solution. The reaction mixture was incubated at room temperature for 1 min. The final concentration of each reagent was 50 μM iron(II), 100 μM EDTA, 0.003% H_2O_2, and 1 mM ascorbate. The reaction was stopped by adding 150 μl of a solution containing 10 mM Tris chloride (pH 8.0), 0.4% sodium dodecyl sulfate (SDS), 15 mM EDTA, 15 mM thiourea, 0.1 M NaCl, and 34 μg of tRNA per ml. The mixture was extracted with 200 μl of phenol followed by 150 μl of phenol-chloroform-isoamyl alcohol. Both organic phases were back-extracted with 200 μl of 10 mM Tris chloride–1.0 mM EDTA (pH 8.0). The aqueous phases were then extracted twice with ether. The products were precipitated twice from ethanol and sodium acetate. The pellet was rinsed with 70% ethanol, dried, and dissolved in 90% formamide containing tracking dyes. After being heated briefly to 90°C, the DNA was electrophoresed in an 8% polyacrylamide–8 M urea sequencing gel (preelectrophoresed so that the gel temperature was between 43 and 46°C) for 4 to 5 h at 50 to 60 W of constant power. The gel was dried and exposed to preflashed film (X-Omat; Eastman Kodak Co.) for 10 days without an intensifying screen.

Analysis of hydroxyl radical footprinting data. Analysis of the footprints was accomplished by densitometric analysis. We scanned each lane of the autoradiograph with a Joyce Loebl Chromoscan 3 densitometer with an aperture width of 0.05 cm. Data points were recorded every 50 μm and stored on the disk of a Macintosh computer so that point-by-point subtractions of the lanes from the same autoradiograph could be performed. The data sets were compressed by removing 2 data points from every 3 to give 1,200 points per 180-mm scan.

A graphing program (Cricket Graph) was used to align, subtract, and graph the data. Two data sets (scans) were plotted together at an expanded scale. Two adjustments were then made to the raw data before subtraction. The first adjustment was removal of up to 10 data points either at the beginning of the data set or at positions between peaks. The other adjustment was multiplication of the entire data set by a constant (usually 0.85 to 1.1). The first adjustment was necessary to ensure that the scans were in phase with one another. Imperfections in the gel cause minute local mobility differences that can easily be corrected in this way. Multiplication by a constant was necessary because the intensity of every lane was not identical. Since the cutting reactions are performed within the limit of one cut per DNA fragment (>75% uncut DNA), this correction is valid (7, 24).

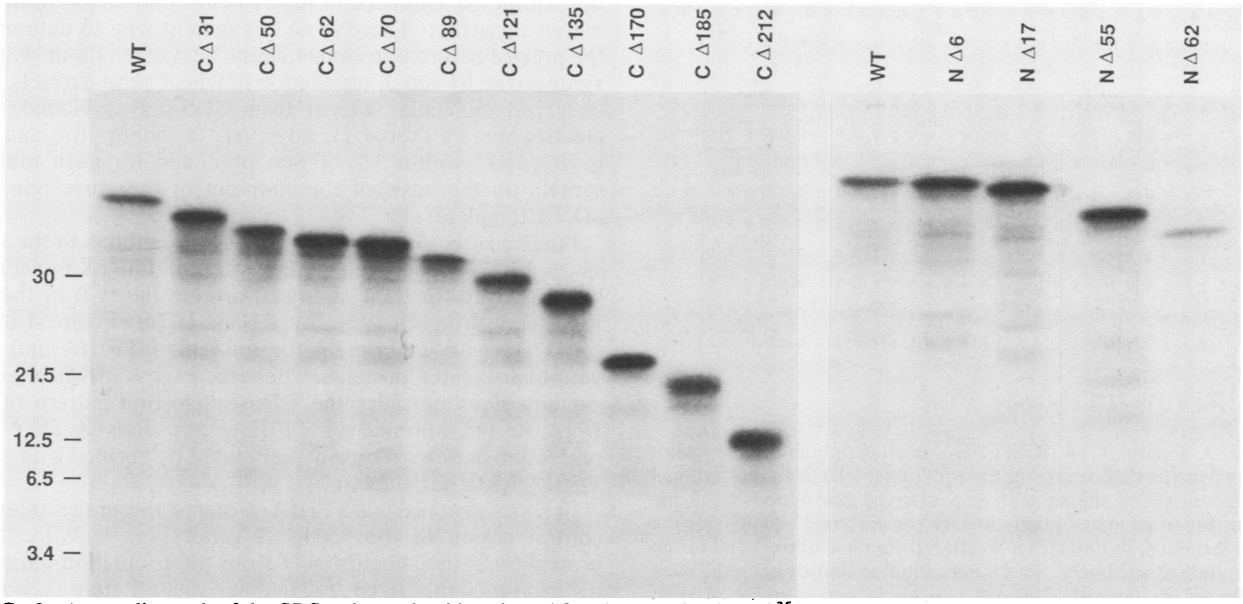

FIG. 2. Autoradiograph of the SDS-polyacrylamide gel used for characterization of ^{35}S-labeled deletion mutants of TFIIIA synthesized in vitro. WT, Wild type. Carboxyl-terminal deletions are prefixed by CΔ, followed by the number of amino acids deleted from that end. The N-terminal deletions are prefixed by NΔ. Position of ^{14}C molecular size standards (in kilodaltons) are given to the left of the figure.

After subtraction, the resulting difference scans were smoothed by computing a running average with a 15-point window, which corresponds to the width of roughly 1.5 peaks. Smoothing reduced the noise resulting from subtraction of imperfectly shaped bands. For the plots resulting from this process, see Fig. 7.

RESULTS

Synthesis of TFIIIA by in vitro transcription of a cloned cDNA and subsequent in vitro translation of the mRNA. Figure 1 depicts the recombinant DNA from which full-length TFIIIA was synthesized and from which mutations in the protein were constructed. A full-length cDNA clone (generously provided by A. Ginsberg and R. Roeder) was subcloned into the *Eco*RI site of pSP65 and called pSPTF15. The construction of the plasmid is such that transcription from the SP6 promoter will produce a messenger RNA composed of 41 nucleotides of 5′ untranslated sequence, 1,035 nucleotides of coding sequence (encoding the 344-amino-acid protein and a stop codon), and 445 nucleotides of 3′ untranslated sequence. The restriction sites shown above the gene in Fig. 1 were used in the construction of deletion mutants (see Materials and Methods).

We have used the procedure of Krieg and Melton (21) for the synthesis of mRNA with SP6 RNA polymerase. Production of translation-competent mRNA was accomplished by including the capped dinucleotide precursor ^{7}mGpppGm in the transcription reaction mixture (Melton, personal communication). Following purification, mRNA was translated in a cell-free wheat germ extract. We monitored the synthesis of the protein by the incorporation of radiolabeled [^{35}S]cysteine because of the abundance of this amino acid in the protein (23 mol of cysteine per mol of TFIIIA). In this manner, we could visualize the synthesized protein in SDS-polyacrylamide gels and also quantitate the molar yield of protein.

An example of full-length radioactive TFIIIA, synthesized in vitro, subjected to SDS-polyacrylamide gel electrophoresis, and subsequently visualized by autoradiography, is shown in Fig. 2 (labeled "WT" in each panel). Coomassie staining of this gel revealed a complex constellation of the abundant wheat germ extract proteins but did not detect newly synthesized protein (data not shown). Excision of the radiolabeled band and quantitation of the yield, on the basis of the specific activity of cysteine, indicates that nanogram amounts of protein were synthesized. A typical yield of newly synthesized protein represents about 1 molecule of protein for every 10 molecules of added mRNA. Radiolabeled TFIIIA synthesized in this reaction migrates in the gel to a position indistinguishable from that of wild-type TFIIIA purified from *X. laevis* ovaries (data not shown). Those radioactive protein bands migrating below full-length TFIIIA are presumed to be due to premature termination of translation, since these bands are present in translation products of full-length, gel-purified TFIIIA mRNA (data not shown), and they change in size in the N-terminal but not the C-terminal deletion series (Fig. 2).

Synthesis of carboxyl- and amino-terminal deletion mutants of TFIIIA. We have constructed a series of shortened genes that give rise to amino acid deletions from either end of the TFIIIA molecule. The translation products of these mutants are shown in Fig. 2. The carboxyl-terminal mutants (labeled CΔ, followed by the number of amino acids removed) were prepared from unique restriction enzyme sites in the TFIIIA gene (Fig. 1) and by exonuclease III-S1 nuclease digestions. For the carboxyl-terminal deletion series, the mRNA was synthesized by runoff transcription, and the protein was then synthesized by runoff translation. This method has been used successfully by Hope and Struhl (20). In the case of the amino-terminal deletions (labeled NΔ, followed by the number of amino acids removed), 5′ sequences were removed (either by restriction endonuclease digestion or exonuclease III-S1 digestion) and replaced with short oligonucleotides containing an initiator methionine codon. Protein synthesis of amino-terminal deletions terminates at the normal translation termination codon in the mRNA.

Figure 3 indicates where each of the deletion endpoints

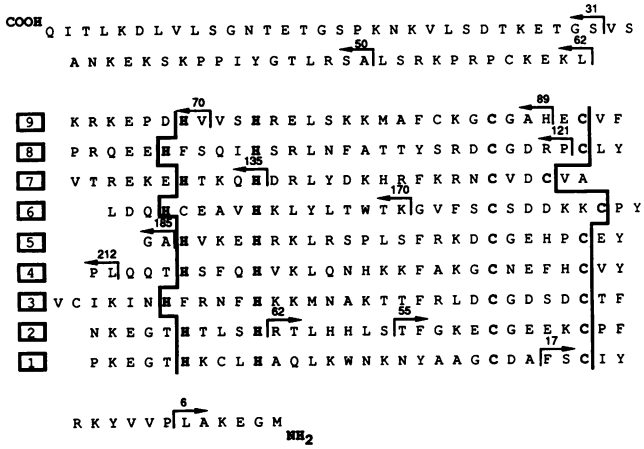

FIG. 3. Positions of the TFIIIA deletion mutants. The entire protein from its carboxyl-terminal end (upper left) to amino-terminal end (lower right) is aligned with respect to the nine hypothetical zinc fingers. When an arrow points toward the carboxyl terminus or the amino terminus, it indicates a deletion from the carboxyl end or the amino end, respectively. The inner histidine and cysteine of each zinc finger are aligned. The outer histidine and cysteine of each finger are demarcated by a thick vertical line. The traditional direction of presenting a protein sequence is reversed here to facilitate comparison with other figures in this paper.

lies within the sequence of the protein as predicted from the cDNA construct. There is no convenient way to determine the precise carboxyl-terminal amino acid of a mutant protein synthesized by runoff translation in wheat germ extract. The observed molecular weight from SDS-polyacrylamide gel electrophoresis (Table 1), however, is within 10% and, in most cases, within 3% of that predicted for each mutant protein on the basis of the endpoint of the corresponding cDNA template.

Binding of in vitro synthesized TFIIIA mutants to the ICR assayed by DNase I footprinting. Mutant TFIIIA molecules were assayed for their ability to protect the ICR of the 5S RNA gene from cleavage by DNase I (14). Figure 4 illustrates such an experiment for full-length TFIIIA and the various truncated proteins. The large excess of wheat germ proteins does not alter the DNase digestion pattern of 5S DNA in the absence of TFIIIA, nor does it alter the protection pattern (footprint) generated by purified wild-type TFIIIA (data not shown).

In vitro synthesized TFIIIA protects the entire internal control region of the 5S RNA gene (Fig. 4, WT). This protection is indistinguishable from the protection afforded by in vivo-synthesized TFIIIA as isolated from *Xenopus* ovaries. The experiment shown in Fig. 4 was performed at a ratio of 5 mol of protein per mol of DNA fragment so as to visualize weaker protein-DNA interactions while still gaining some insight into the relative binding strengths.

Inspection of the carboxyl-terminal deletion series shows that the protein extends along the DNA, with its carboxyl

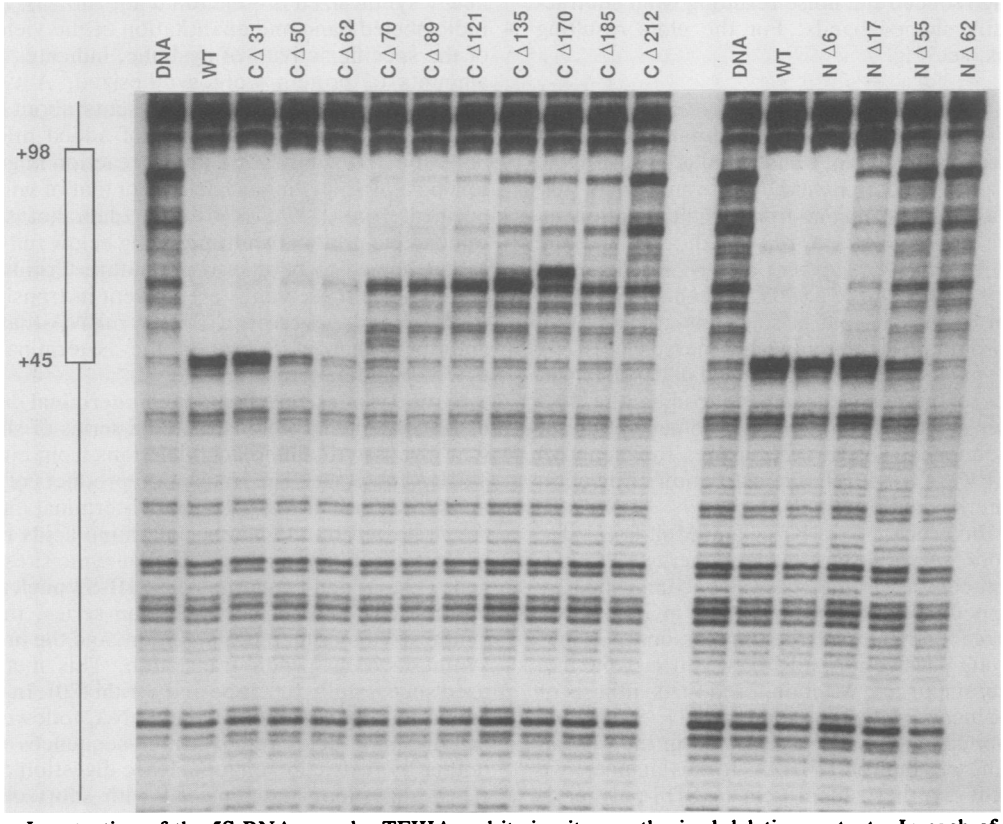

FIG. 4. DNase I protection of the 5S RNA gene by TFIIIA and its in vitro-synthesized deletion mutants. In each of these assays, the TFIIIA concentration (as determined by quantitating [^{35}S]cysteine incorporation during the translation reaction) was controlled to give a ratio of five protein molecules for each 5S RNA gene (Xbs201). The position of the ICR of the 5S RNA gene is shown next to the footprint. The coding strand of the 5S RNA gene was footprinted. Abbreviations and designations are defined in the legend to Fig. 2.

end toward the 5′ end of the ICR and its amino terminus toward the 3′ end. Deletion of the first 50 amino acids from the carboxyl terminus does not change the number of nucleotides protected from DNase I. However, removal of the amino acids from CΔ31 to CΔ50 does cause the loss of a DNase I hypersensitive site at the 5′ border of the ICR. The identical change has been described from the footprint of the 30-kilodalton proteolytic fragment of TFIIIA (42). We will show that this deletion, with only this subtle effect on DNA binding, reduces the ability of TFIIIA to support transcription of 5S RNA by about 90% (see Fig. 9) just as for the 30-kilodalton proteolytic fragment (42).

The first major change in DNase I protection occurs between the footprints of CΔ62 and CΔ70. The former delimits the border of the DNA-binding domain just before zinc finger 9 and generates a full footprint weakened at the 5′ end. The latter construct deletes eight additional amino acids, including the outer histidine of zinc finger 9. As a result of the deletion of these eight amino acids, the footprint over the 5′ one-third of the ICR is lost (nucleotides +45 to +63). Although the 5′ portion of the ICR is no longer protected, there is some interaction remaining, as shown most clearly by new hypersensitive sites in the footprint of the deletion mutant CΔ70.

This partial protection pattern remains about the same with further deletions from the carboxyl terminus that extend into zinc fingers 8, 7, and 6 (CΔ89 through CΔ185). Furthermore, progressive deletions weaken overall binding which is apparent in the gradual loss of protection throughout the 3′ end of the ICR. Deletion of approximately 60% of the amino acids from the carboxyl terminus, through zinc finger 5 (CΔ212), produces a protein that does not protect the ICR from DNase I. Increasing the molar ratio of protein to DNA fragment from 5:1 (Fig. 4) to 20:1 increases the protection of the 3′ end of the ICR by carboxyl mutants CΔ121 through CΔ185 without producing any evidence for the binding of CΔ212 to the gene (data not shown). However, weak binding of CΔ212 to the ICR was detected by hydroxyl radical footprinting (see below).

We next turned our attention to the binding characteristics of the amino-terminal deletion mutants. Removal of six residues from the amino terminus (NΔ6), with the obligatory addition of an initiator methionine, produces a protein that appears to be wild type in its binding to the gene (Fig. 4, NΔ6). However, deletion of 17 amino acids (NΔ17) reduces the binding affinity of the protein over the entire length of the ICR. This mutant results from deletion of the amino-terminal end of the DNA-binding domain of TFIIIA to the beginning of zinc finger 1. As with the carboxyl-terminal series, protection of the ICR could be enhanced by increasing the ratio of the mutant protein to DNA (data not shown). At higher protein concentrations the next mutant, NΔ55, weakly protects the ICR from DNase I, and NΔ62 does not bind detectably in this assay even at higher protein concentrations.

Hydroxyl radical footprint of TFIIIA bound to the 5S RNA gene. DNase I footprinting does not give an unbiased view of protein-DNA interactions. The well-documented sequence preferences of DNase I cause nonrandom cleavage of naked DNA. Furthermore, the ability of DNase I to cleave a DNA-protein complex is limited by the size of the enzyme and by the fact that it cleaves across the minor groove (11). Therefore, we turned to a high-resolution chemical footprinting method to study the TFIIIA deletion mutants. The hydroxyl radical (·OH), generated by the reduction of hydrogen peroxide by iron(II) EDTA (the Fenton reaction), cleaves DNA relatively nonspecifically (45). Cleavage is effected by abstraction of a hydrogen atom from a deoxyribose residue in the DNA backbone. The resulting sugar radical then decomposes to give a single-strand gap at the point of hydroxyl radical attack. The presence of a bound protein lowers the probability of cleavage of the DNA by hydroxyl radical at the protein-binding site, thereby generating a footprint (45, 46).

The hydroxyl radical method gives information on protein contact for every nucleotide in the binding site because each sugar-phosphate bond is cleaved to some extent by the hydroxyl radical. Since the hydroxyl radical cleaves DNA by reacting with the sugar-phosphate backbone, sites of protection by bound protein correspond to places where the protein shields the backbone from the solvent. Sequence-specific hydrogen-bonding contacts of a protein with the DNA bases exposed in the major groove do not necessarily result in protection from hydroxyl radical attack, as was shown for lambda repressor and Cro protein (45). Since the protection pattern reflects proximity of the protein to the sugar-phosphate backbone, the pattern may not reflect the nucleotide interactions most responsible for specificity of protein binding.

Figure 5 shows an autoradiograph that compares DNase I and hydroxyl radical footprints of TFIIIA on the coding and noncoding strands of the 5S RNA gene. This experiment was designed so that the band corresponding to a nucleotide on one strand is adjacent, on the autoradiograph, to the complementary nucleotide on the other strand. The two footprinting methods gave slightly different boundaries for the ICR; within the ICR, the enhanced resolution of hydroxyl radical cleavage was apparent. The two DNase I hypersensitive sites near the center of the ICR on the noncoding strand appeared as poorly protected regions in the hydroxyl radical footprint. The coding strand, which had no DNase I cleavages within the ICR, had a pattern of protection and exposure to the hydroxyl radical that was similar to the pattern of the noncoding strand but offset by about 3 nucleotides.

Inspection of the hydroxyl radical footprints in Fig. 5 (lanes 6 to 9) shows broad protection at either end of the ICR for more than one turn of the helix: +42 to +60 at the 5′ end and +78 to +97 at the 3′ end. It appears that the protein is in intimate and uninterrupted contact with one to two helical turns of DNA at either end of the ICR. The protection pattern in the center of the ICR is quite different. Here the protein seems to lie on the surface of one side of the DNA helix, much as has been described for bacteriophage repressors on their cognate sequences (1). This pattern is characterized by protection of a few nucleotides centered at position +64 on the coding strand and protection of the same number of nucleotides on the noncoding strand at position +67. The 3-nucleotide offset of protection suggests that the protein binds across the minor groove at the center of the ICR (45). This protected region is separated by roughly one turn of the helix (10 to 12 base pairs) from the broad regions of protection at the ends of the ICR.

Hydroxyl radical footprinting of deletion mutants of TFIIIA with the ICR. Figure 6 illustrates hydroxyl radical footprints of TFIIIA and the deletion mutant series on the 5S RNA gene. In contrast to the apparent stepwise loss of protection seen with DNase I, the chemical reagent reveals a progressive loss from the 5′ end to the center of the ICR for the carboxyl-terminal deletion series. This is best analyzed by comparing densitometer tracings of each footprint (Fig. 7). The striking result is that removal of a small number of

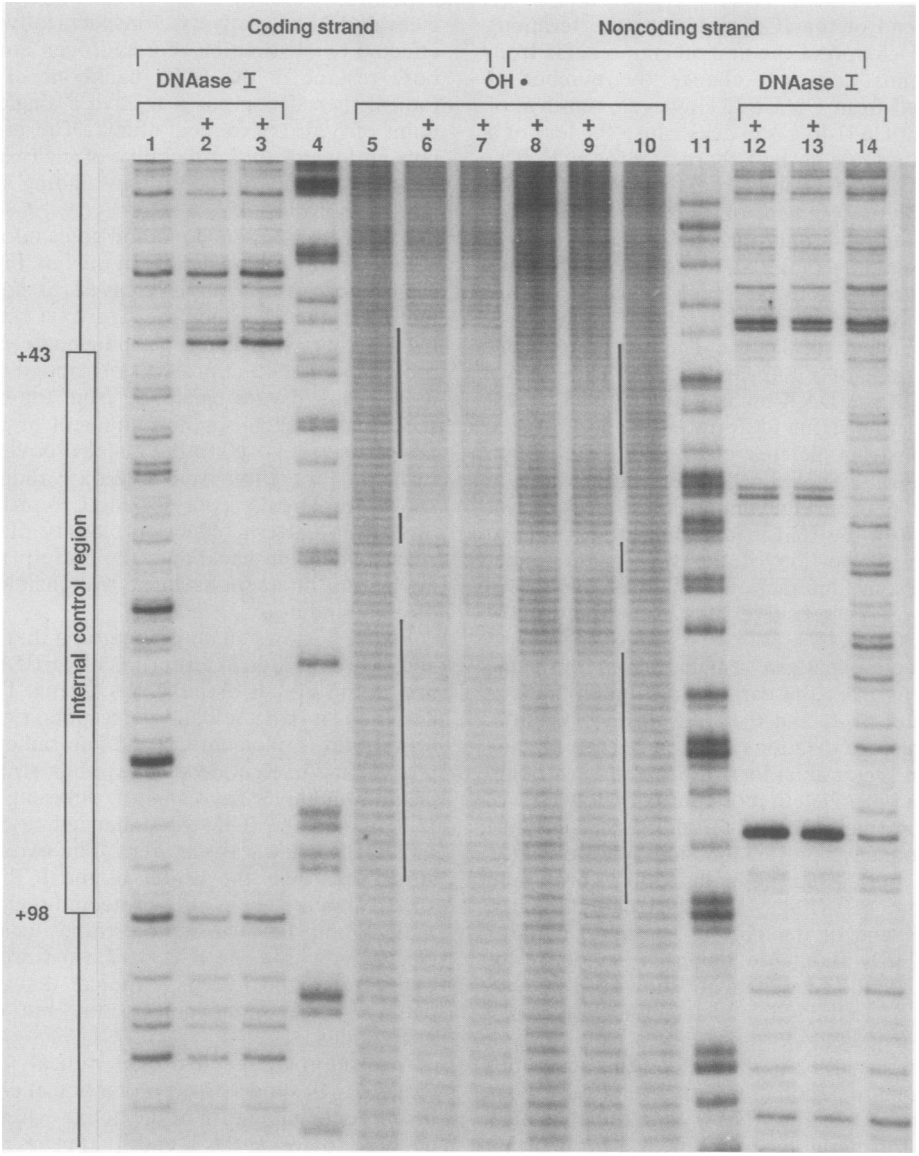

FIG. 5. Hydroxyl radical and DNase I footprints of TFIIIA on the 5S gene. This autoradiograph compares hydroxyl radical and DNase I footprints for each strand of the 5S RNA gene pXbs201. End-labeled DNA was incubated with and without TFIIIA as described in Materials and Methods. The coding (lanes 1 to 7) and noncoding (lanes 8 to 14) strands are aligned so that adjacent bands are at the same position in the sequence. Products of DNase I digestion of the 5S RNA gene with bound TFIIIA are shown in duplicate (lanes 2, 3, 12, and 13), and those without protein are in lanes 1 and 14. Products of hydroxyl radical cleavage of 5S RNA with bound TFIIIA are shown in duplicate (lanes 6, 7, 8, and 9), and those without protein are shown in lanes 5 and 10. Lanes 4 and 11 show the guanine-specific cleavage marker lanes. The marker to the left shows where the ICR is in relation to the footprints. The lines between lanes 5 and 6 and lanes 9 and 10 delineate the three regions that are protected from hydroxyl radical cleavage.

amino acids had a localized effect on the footprint. This effect was so localized that we can project each amino acid region over its cognate DNA within the ICR. The hydroxyl radical footprints of the carboxyl deletion series also illustrate the effect of progressive deletions on the overall binding energy which we observed in the DNase I protein experiment (Fig. 4). The most extreme carboxyl-terminal mutant in our series for which the hydroxyl radical footprinting method detected binding was CΔ212.

The amino-terminal deletion series also shows a progressive loss of the footprint but now moving from the 3′ end of the ICR toward the 5′ end (Fig. 6 and 8). The hydroxyl radical footprint demonstrates local loss of protein-DNA contact at the 3′ end of the ICR caused by deletion into the first zinc-binding domain (NΔ17) along with the overall general weakening of binding observed in the DNase I footprint (Fig. 4). This phenomenon was seen for two deletions into the DNA-binding domains NΔ17 and NΔ55. No binding was detected for the next deletion in the series, NΔ62.

To visualize the contributions of individual zinc fingers to the hydroxyl radical footprint, we developed a difference method for analysis of footprint data of the TFIIIA deletion mutants. A densitometer scan of the footprint of one mutant is subtracted point by point from a scan of the footprint of a longer mutant. The deletion mutants chosen for analysis differ in length by nearly integral numbers of zinc fingers. The resulting difference plots were smoothed by computer

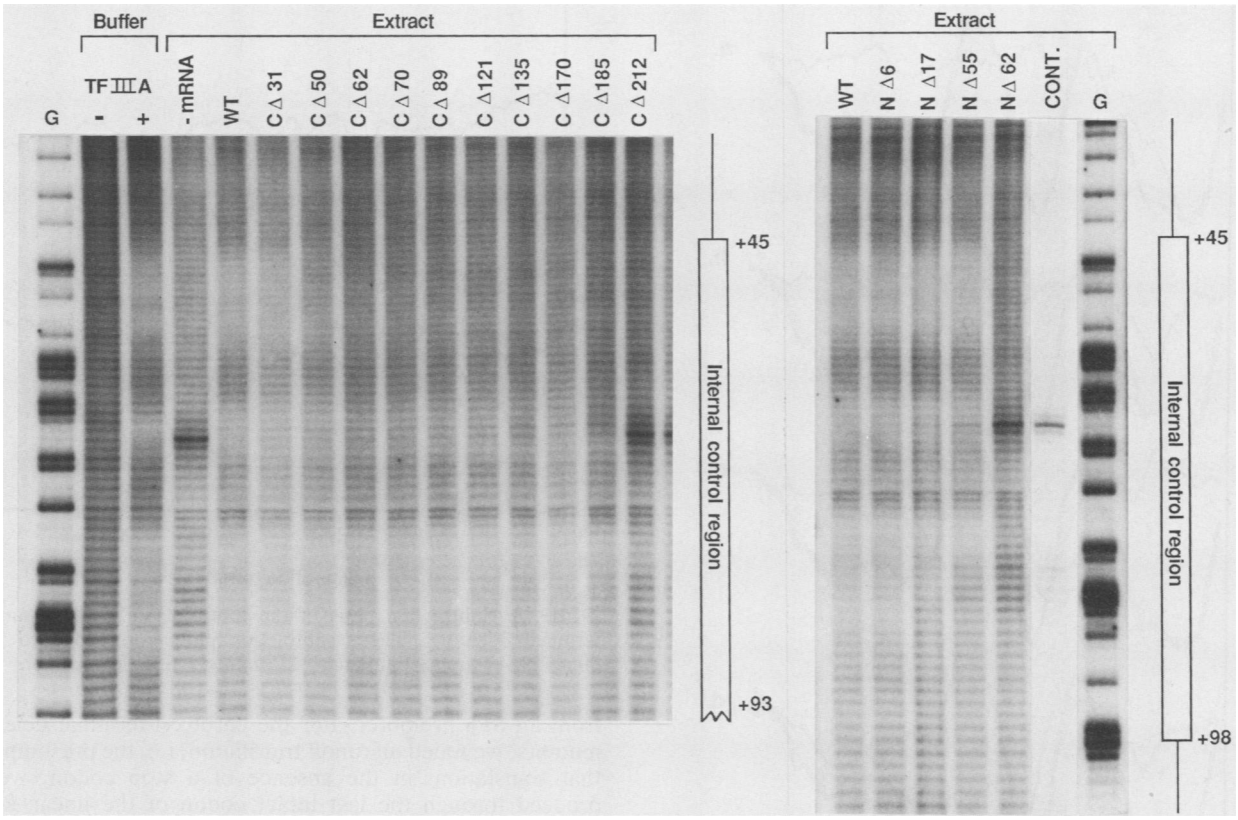

FIG. 6. Hydroxyl radical footprints of the TFIIIA deletion mutants. This autoradiograph shows the footprints of the carboxyl- and amino-terminal deletion series on the noncoding strand of pXbs201. The lanes represent DNA cleaved by hydroxyl radical in buffer (−); DNA with bound TFIIIA cleaved by hydroxyl radical in buffer (+); DNA cleavage pattern in wheat germ extract without mRNA added (−mRNA); footprints of in vitro synthesized TFIIIA (WT) and of the carboxyl deletion series in wheat germ extract; in vitro synthesized TFIIIA (WT) and the amino-terminal deletion series (loaded at a different time, hence the offset of the protection patterns); cleavages caused by incubation of DNA alone in the extract (CONT.); and G-specific cleavage reaction of pXbs201 (G). The extent of the ICR is diagrammed to the right of each autoradiograph.

for clarity (see Materials and Methods) and plotted along with the smoothed footprint of wild-type TFIIIA for comparison. The amino-terminal mutants also were analyzed by this method (Fig. 8).

The difference plots represent the loss of protection that occurs because of the deletion of one or more zinc fingers from the protein. It is clear from Fig. 7 that the loss of DNA protection with each deleted protein domain was progressive along the DNA from 5′ to 3′ and restricted to a local region just a few base pairs in length. This was accompanied by weakening of the overall binding energy of the protein to the ICR. The actual region of the ICR locally protected by each region of TFIIIA is summarized in the Discussion (see Fig. 10).

In vitro-synthesized TFIIIA supports transcription of a cloned 5S RNA gene. In addition to assays for sequence-specific DNA binding, we have tested TFIIIA and its deletion mutants for their ability to support the in vitro transcription of a cloned 5S RNA gene. For these experiments, a transcription extract prepared from *Xenopus* oocytes (4) was immunologically depleted of TFIIIA with a polyclonal antiserum and protein A-Sepharose. This procedure produces an extract that will no longer support transcription of 5S RNA genes but remains competent to support transcription of tRNA genes. Transfer RNA genes share factors other than TFIIIA with 5S RNA genes, and both kinds of genes are transcribed by RNA polymerase III (22). As with the footprinting studies, these experiments were made possible by the fact that the wheat germ translation reaction mixture does not interfere with the in vitro 5S RNA transcription reaction. We could, therefore, add crude wheat germ extract containing in vitro-synthesized TFIIIA (or a mutant protein) directly to the depleted *Xenopus* oocyte transcription extract and test the ability of this crude mix of extracts to reconstitute synthesis of 5S RNA from a cloned 5S RNA gene.

The "CONTROL" lanes in Fig. 9 show the result of transcribing a tRNA and a 5S RNA gene in the TFIIIA-depleted extract. In the absence of TFIIIA, the 5S RNA gene is not transcribed. Synthetic TFIIIA ("WT" in Fig. 9) reconstitutes approximately 70% of the transcription that is observed in an identical mixture of extracts to which the same amount of TFIIIA isolated from *Xenopus* ovaries was added (data not shown). It is unclear why synthesized TFIIIA does not function identically to TFIIIA isolated from *Xenopus* ovaries. Perhaps one reason is competitive inhibition caused by the shorter proteins that result from premature translation termination (Fig. 2). The reduction in tRNA transcription in the presence of TFIIIA is thought to be due to the fact that transcription factors shared by 5S RNA and tRNA genes (TFIIIB or TFIIIC or both) are present at limiting concentrations and that under these conditions the two genes compete for these molecules (31).

Removal of the carboxyl-terminal 31 amino acids from TFIIIA had no effect on 5S RNA synthesis, but removal of

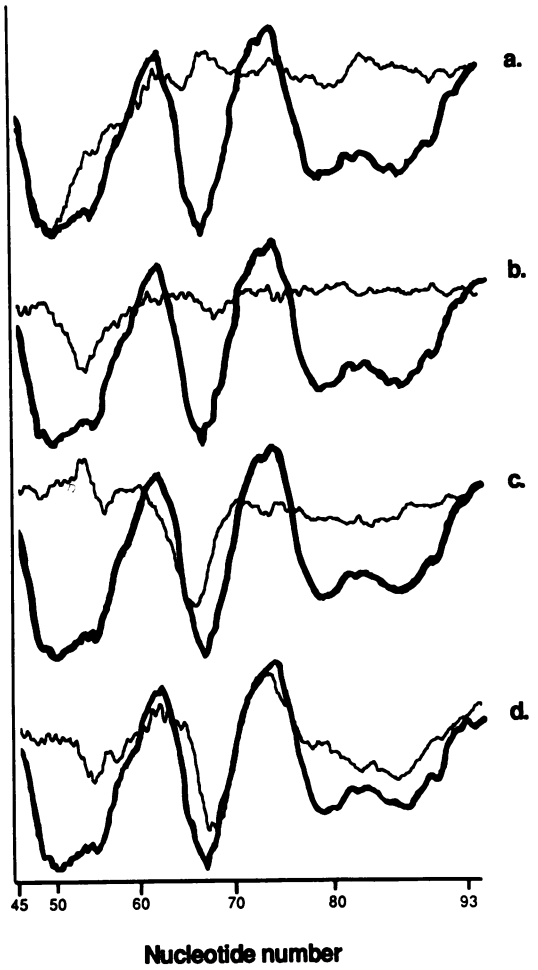

FIG. 7. Subtraction plots of the footprints of pairs of carboxyl-terminal deletions. The thin graph line dips over those base pairs of the ICR protected differentially in the longer mutant. Lines a, Wild-type minus CΔ89 (shows protection by finger 9); lines b, CΔ89 minus CΔ121 (shows protection by finger 8); lines c, CΔ121 minus CΔ185 (shows protection by fingers 6 and 7); lines d, CΔ185 minus CΔ212 (shows protection by finger 5). The bold line in each plot is the trace of a wild-type TFIIIA footprint of the noncoding strand.

an additional 19 amino acids (CΔ50) reduced 5S RNA transcription by nearly 90%. This low level of transcription was unchanged with progressive deletions through CΔ121, at which point mutant proteins no longer complemented the depleted extract and supported 5S RNA transcription.

Similar analyses were conducted for the amino-terminal deletion series (Fig. 9). Unlike the carboxyl-terminal deletion series, there was a close correlation between the loss of the ability of a particular mutant protein to support transcription and the loss of its binding affinity to the ICR. We conclude that there is no evidence for a specific transcription domain at the amino terminus of the protein; rather, the transcription efficiency of amino-terminal mutants depends upon DNA-binding affinity.

DISCUSSION

Runoff transcription and runoff translation generate functional TFIIIA and deletion mutants. We have used linear DNA molecules as templates for synthetic mRNAs initiated

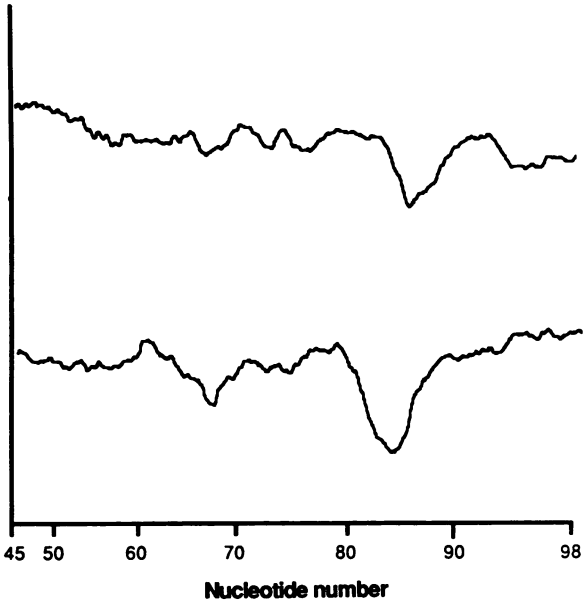

FIG. 8. Subtraction plots of the footprints of pairs of amino-terminal deletions. These subtraction plots correspond to NΔ6 minus NΔ17 (upper line) and NΔ17 minus NΔ55 (lower line).

from an SP6 promoter. For the carboxyl-terminal deletion mutants, we relied on runoff translation, i.e. the presumption that translation, in the absence of a stop codon, would proceed through the last intact codon of the linear RNA molecule. The evidence we have to support this presumption is the agreement of the size of proteins synthesized in vitro with their predicted size, as measured by their mobility in gel electrophoresis relative to known proteins (Table 1).

Even if we did know the precise size of each mutant protein, interpretation of the results assumes that a particular deletion mutant has no global effect on protein function by altering some important tertiary structure. As an example, consider the general loss of binding affinity observed for the small amino-terminal deletion NΔ17 (Fig. 4). This substantial loss in binding affinity could be due to either a general perturbation of the mutant protein tertiary structure or the loss of a few local amino acid-nucleotide interactions which, in turn, destabilize the protein binding to the ICR. Previous mutation and deletion studies of the ICR strongly support the latter interpretation. It is the excellent agreement of the behavior of these protein mutants with the published analysis of ICR mutants that gives us confidence in our interpretation of the experiments reported in this paper.

This particular system of in vitro transcription and translation was chosen after unsuccessful attempts to prepare functional TFIIIA in *E. coli* or by translation in reticulocyte lysates. In *E. coli*, we found that full-length TFIIIA was often partially degraded, and a substantial fraction of the protein was insoluble. Reticulocyte lysates do not produce immunoprecipitable TFIIIA (W. Taylor, unpublished data). Wheat germ extract is remarkably benign in the two assays we used to examine the function of in vitro-synthesized TFIIIA. The extract does not inhibit footprinting of a 5S RNA gene by TFIIIA that is present at less than 0.01% of total protein. When combined with oocyte nuclear extract to test complementation of transcription, wheat germ extract neither inhibits the reaction nor contributes components that might confuse the complementation assay for functional

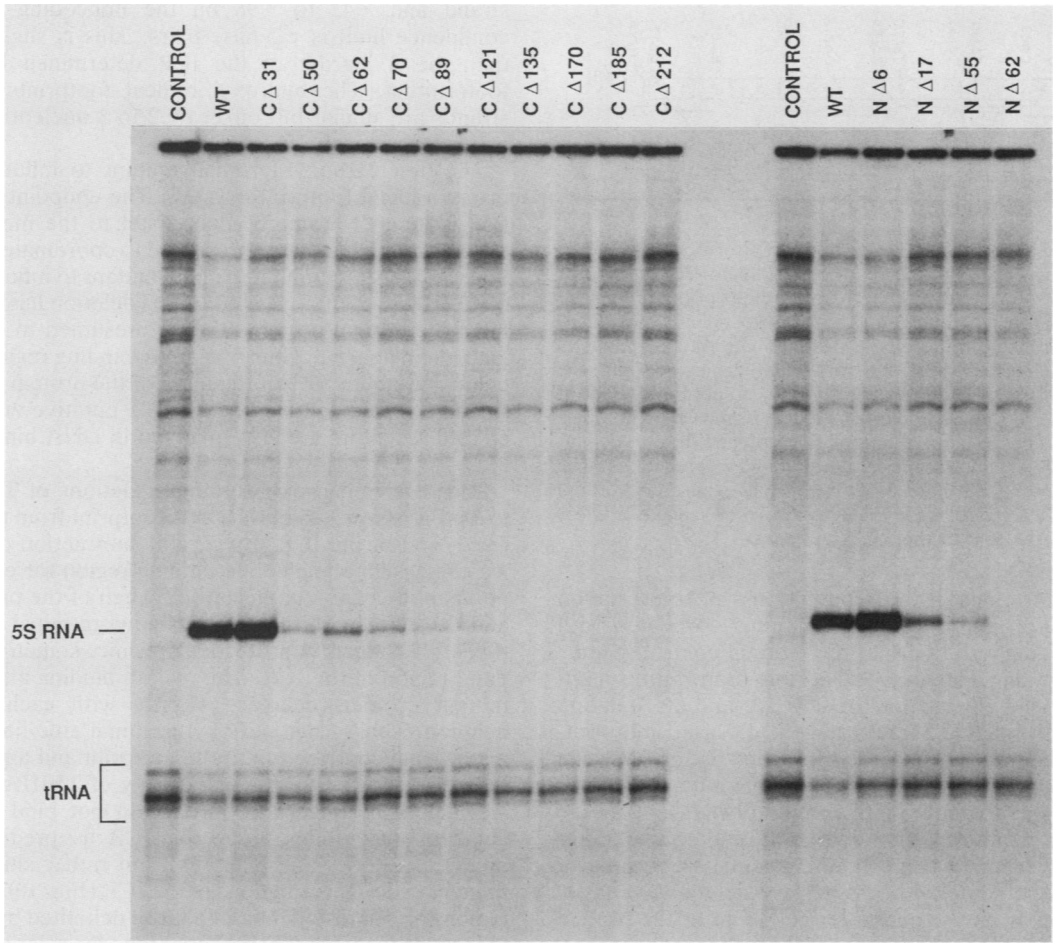

FIG. 9. Autoradiograph of transcription products obtained by supplementing a TFIIIA-depleted oocyte nuclear transcription extract with in vitro-synthesized TFIIIA or its deletion mutants. The plasmids for transcription (pXbs201 and pXltmet) were maintained at a concentration of 1 μg/ml, and the total DNA concentration was brought to 10 μg/ml with pSP65. In vitro-synthesized TFIIIA or a mutant was added directly to the transcription extract (in the wheat germ translation extract) at a concentration such that the ratio of protein to 5S RNA gene was 5:1. The migration positions for 5S RNA and the tRNA products are illustrated in the figure. The control reaction contained wheat germ translation extract lacking TFIIIA. WT, TFIIIA synthesized in vitro from full-length mRNA. Identification of all other lanes is the same as in the legend to Fig. 2.

TFIIIA. Similar conclusions permitted Hope and Struhl (20) to study the DNA-binding properties of mutants of the yeast *trans*-acting factor GCN4.

The transcription domain. Previously we had shown that a proteolytic product of TFIIIA binds to the ICR as tightly as full-length TFIIIA but has lost about 90% of the ability of native TFIIIA to complement transcription (42). In the present experiments, we have refined the location of this transcription domain (Fig. 9 and 10). Loss of the first 31 amino acids from the carboxyl terminus has no effect on transcription, but deletion of just 19 amino acids more causes a loss of transcription complementation of greater than 90%. Little if any effect on DNA binding, as assayed by the two footprinting methods, occurs as a result of this deletion. We presume that these 19 amino acids (positions 32 through 50 from the carboxyl terminus) constitute part of a polypeptide region that interacts with RNA polymerase III or with TFIIIB and/or TFIIIC, the other essential transcription factors that are required to form the transcription complex.

Whereas a region near the carboxyl terminus, outside the DNA-binding region, influences transcription initiation on a 5S RNA gene, no specific transcription domain was detected

TABLE 1. Predicted and expected molecular weights for TFIIIA deletion mutants synthesized in vitro

Protein	Mol wt		Additional amino acids
	Predicted	Observed	
TFIIIA	39,750	39,000	
CΔ31	36,611[a]	37,000	Ser
CΔ50	34,773[a]	35,000	Gly Pro Ala Ala
CΔ62	33,493[a]	34,000	Asp Leu Gln Pro
CΔ70	32,537[a]	33,000	Val Thr Cys Ser Pro
CΔ89	29,978	32,000	
CΔ121	26,169	29,000	
CΔ135	25,251[a]	26,000	Gly
CΔ170	20,272[a]	22,000	Lys
CΔ185	18,656[a]	19,000	Ala
CΔ212	15,322	15,000	
NΔ6	39,234	39,000	
NΔ17	37,879	37,000	
NΔ55	33,683	34,000	
NΔ62	32,839	32,000	

[a] These predicted molecular weights include non-TFIIIA-encoded amino acids at the carboxyl terminus which have been transcribed and translated from polylinker sequences. These additional amino acids are listed in the last column.

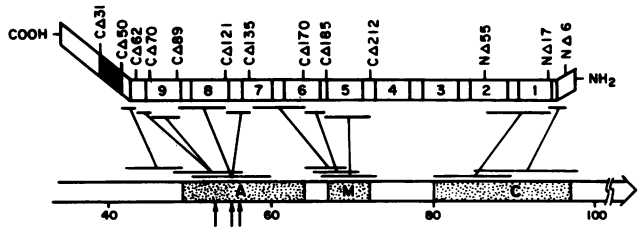

FIG. 10. Alignment of TFIIIA along the ICR of a 5S RNA gene. The nine zinc fingers are shown separated by linkers. The location of each deletion is shown above the protein. Regions of the protein (at either end) that are not involved in binding to the ICR are tilted upwards. The transcription domain near the carboxyl terminus is shaded. The deleted part of the protein is projected onto the protected part of the ICR that is identified by a subtraction plot of the two hydroxyl radical footprints (Fig. 7 and 8). The lines extending from TFIIIA (above) to the 5S RNA gene (below) delimit three regions, A, M, and C (see Discussion and reference 33). The three vertical arrows are base pairs in the ICR where oocyte and somatic 5S RNA genes differ. TFIIIA is drawn to scale as a linear molecule above the ICR of the 5S RNA gene.

at the amino terminus of the protein. Loss of transcription with progressive amino-terminal deletions correlates with weakened binding of TFIIIA to the internal control region.

The DNA-binding domain. We used two footprinting methods to study the interaction of TFIIIA and its deletion mutants with the ICR. The advantage of DNase I footprinting lies in the completeness of the protection pattern. We can compare the strength of binding of various mutant proteins by following the extent of protection to DNase I in the footprint. For example, when the carboxyl-terminal footprint series is scanned (Fig. 4), the gradual weakening of overall TFIIIA binding with progressive deletions is easily seen. Deletions from the amino-terminal end of the protein cause rapid loss of overall binding affinity.

We believe that the hydroxyl radical footprint gives the truest representation of the proximity of amino acids within TFIIIA to nucleotide residues in the ICR. Here the effect of a protein deletion can be assessed at every base pair within the ICR. The progressive loss of the hydroxyl radical-generated footprint with each succeeding deletion mutant (Fig. 6 to 8) contrasts with the stepwise appearance of the same series with DNase I (Fig. 4). DNase I has an affinity of its own for DNA and can displace weak protein-DNA interactions by competition for the binding site. The hydroxyl radical footprinting method avoids this artifact. However, the hydroxyl radical method does not sense the binding of an alpha helix or possibly even a zinc finger in the major groove unless there is also an additional interaction which carries over to the phosphate-sugar backbone.

Results from both sets of TFIIIA deletions agree with previous studies that analyzed deletion and point mutants of the ICR. Deletions into the 5′ end of the ICR (box A in Fig. 10) progressively shorten the TFIIIA footprint in the 5′-to-3′ direction (39). Point mutations within the 5′ part of the ICR confirm the importance of this region (27, 33). 5′ deletion mutants beyond nucleotide +70 drastically weaken binding of TFIIIA (39). This is almost certainly due, in part, to critical nucleotides centered at +70 and +71 that are required for binding TFIIIA (33, 38; box M in Fig. 10). Deletions (5) and point mutations (27, 32) in the 3′ end of the ICR between +80 and +90 (box C in Fig. 10) have delimited nucleotide residues critical for TFIIIA binding (38).

The limits of TFIIIA contact to the ICR determined by hydroxyl radical footprinting are +40 to +96 on the coding strand and +42 to +98 on the noncoding strand. The confidence limit is ±2 base pairs. This is slightly different than the 5′ border of the ICR determined by DNase I footprinting. The hydroxyl radical footprints of the two strands are similar but offset by 2 to 3 nucleotides over the entire length of the ICR (Fig. 5).

The first carboxyl-terminal mutant to influence the hydroxyl radical footprint is CΔ62. The endpoint of this deletion is located 6 amino acids distal to the most carboxyl-terminal histidine that is presumed to coordinate a zinc ion in finger 9. The first amino-terminal mutant to influence binding of TFIIIA to the ICR is NΔ17. This deletion has removed the most N-terminal cysteine that is presumed to coordinate a zinc ion in finger 1. Thus, the DNA-binding region of TFIIIA composes about 80% of the mass of the protein and includes the nine repeating zinc fingers. The putative zinc fingers of steroid receptors are also involved in DNA binding (15, 17, 35).

Progressive carboxyl-terminal deletions of TFIIIA result in a progressive loss of the DNA footprint from the 5′ toward the 3′ end of the ICR. By careful subtraction of footprints, we can assign a nucleotide-binding region for each adjacent polypeptide region in the carboxyl half of the protein (Fig. 7 and 10). Each of the five carboxyl-terminal zinc fingers (fingers 5 though 9) protects a specific, sometimes overlapping, region of the ICR. The overall binding affinities of the mutant proteins decrease slightly with each subsequent deletion. Thus, each carboxyl-terminal zinc finger makes a major local contribution to the footprint and a minor contribution to the overall binding energy of TFIIIA to the ICR. Adjacent zinc fingers in TFIIIA do not bind to precisely adjacent nucleotides along the ICR as predicted by the model of Rhodes and Klug (34), but rather clusters of zinc fingers bind to three regions of the ICR (Fig. 10). These three regions are almost identical to those delimited by Pieler et al. (33) as critical for TFIIIA function, by a large number of point mutations and deletion mutants within the ICR. These three regions are seen in the tripartite shape of the hydroxyl radical footprint (Fig. 5 and 7), which shows that TFIIIA interacts with at least one full turn of the helix at each end of the ICR (boxes A and C) and binds across the minor groove of the DNA at the center of the ICR, the middle region we will call box M.

The following general model of how TFIIIA binds to the ICR takes into account the data presented here along with previously published work from the several laboratories referred to throughout this paper. The largest contribution to the binding energy is due to the interaction of the two zinc fingers closest to the amino terminus (fingers 1 and 2) with a sequence of about 17 base pairs (+80 to +97) at the 3′ end of the ICR (region C in Fig. 10). We presume that the protein is in intimate contact in the major groove with almost every nucleotide through at least one turn of the DNA helix, including each of six critical G residues on the noncoding strand of the DNA (38). The protein emerges from the major groove at about nucleotide +80 to lie on one side of the DNA for about 20 base pairs. The protein, through zinc fingers 5 and 6, contacts and protects the ICR across the minor groove (region M in Fig. 10), yet in doing so it makes critical contacts in the major groove with adjoining nucleotides, including the two G residues +70 and +71 (38). Proceeding toward the carboxyl end of TFIIIA and toward the 5′ end of the ICR, the protein then appears once again as it did in the C region to bind intimately with the ICR for about 20 base pairs of DNA (nucleotides +42 to +60 or box A; 33). This binding is mediated through zinc fingers 8 and 9 and also by

a short polypeptide region on the carboxyl side of zinc finger 9. This DNA-binding region, delimited by the deletion mutants CΔ50 and CΔ62, may be in fact functionally equivalent to a linker region between fingers (40). Because deletion into finger 2 abolishes binding, we did not assess the binding of zinc fingers 3 or 4 in this study.

Although the footprint of box A resembles superficially that of box C, these two regions differ quantitatively (that is, in binding strength) and probably qualitatively (that is, in their functional role in a transcription complex). Quantitative binding differences have already been described. They can be summarized by pointing out that carboxyl-terminal fingers 5 to 9 have much more pronounced local effect on binding to boxes A and M than they do on the overall binding energy of TFIIIA to the ICR, while the amino-terminal fingers (1 and 2) that bind box C are just the opposite. Box A is greatly influenced by and influential in transcription complex formation (33), and it is through TFIIIA binding to box A that the differential expression of oocyte and somatic 5S RNA genes appears to be mediated. We have noted the effect of three base changes in box A (vertical arrows in Fig. 10) that distinguish the oocyte from the somatic 5S RNA gene (9). The integrity of both the 5′ end of the ICR (37) and the carboxyl terminus of TFIIIA (Fig. 9) is essential to support transcription initiation by RNA polymerase III. Evidence is accumulating that TFIIIC interacts with box A (33). Thus, zinc finger 9, and perhaps 8 as well, anchors TFIIIA to box A of the ICR, an event essential for transcription complex formation.

The modular zinc finger structure allows the protein to extend so that it covers a rather large DNA-binding site (270 amino acids bind to 56 base pairs). TFIIIA has three important contact points along the DNA which are made much stronger when the protein is part of a functional transcription complex. We have argued that the biological significance of a nucleoprotein complex in a eucaryotic nucleus is its stability (6, 8) which is demonstrated in part by an ability to withstand but not impede the passage of RNA polymerase (23, 47). The multiple contacts needed for binding stability may be generated through an elongated single protein such as TFIIIA or an aggregate of proteins such as a nucleosome that interacts with a long stretch of DNA. Alternatively, proteins, with separate DNA-binding sites perhaps quite distant from one another, could touch each other forming a transcription complex. Judging from the multiplicity of control elements upstream and within almost any given protein gene that has been studied in eucaryotes (25, 28), this latter method of transcription complex formation and stability emerges as an attractive mechanism for controlling genes encoding proteins.

ACKNOWLEDGMENTS

This paper was improved by the comments of M. Andrews, J. Berg, E. Crawford, M. Darby, S.-H. Kim, C. Pabo, A. Wolffe, and Y. Yaoita. We thank W. Taylor for a gift of DNA clones and for his instruction in the preparation and use of wheat germ extracts. A. Ginsberg and R. Roeder kindly provided us with a cDNA clone.

The research was supported in part by Public Health Service grants from the National Institutes of Health to D.D.B. and T.D.T. and by the Searle Scholars Program of the Chicago Community Trust (T.D.T.). K.E.V. was the recipient of a National Research Service Award.

LITERATURE CITED

1. **Anderson, J. E., M. Ptashne, and S. C. Harrison.** 1987. Structure of the repressor-operator complex of bacteriophage 434. Nature (London) **326**:846–852.
2. **Bencini, A. A., G. A. O'Donovan, and J. R. Wild.** 1984. A protocol for rapid chemical degradation sequencing. Biotechniques **2**:4–5.
3. **Bieker, J., and R. G. Roeder.** 1984. Physical properties and DNA-binding stoichiometry of a 5S gene-specific transcription factor. J. Biol. Chem. **259**:6158–6164.
4. **Birkenmeier, E. H., D. D. Brown, and E. Jordan.** 1978. A nuclear extract of Xenopus oocytes that accurately transcribes 5S RNA genes. Cell **15**:1077–1086.
5. **Bogenhagen, D. F., S. Sakonju, and D. D. Brown.** 1980. A control region in the center of the 5S RNA gene directs specific initiation of transcription. II. The 3′ border of the region. Cell **19**:27–35.
6. **Bogenhagen, D. F., W. M. Wormington, and D. D. Brown.** 1982. Stable transcription complexes of Xenopus 5S RNA: a means to maintain the differentiated state. Cell **28**:413–421.
7. **Brenowitz, M., D. F. Senear, M. A. Shea, and G. K. Ackers.** 1986. "Footprint" titrations yield valid thermodynamic isotherms. Proc. Natl. Acad. Sci. USA **83**:8462–8466.
8. **Brown, D. D.** 1984. The role of stable complexes that repress and activate eukaryotic genes. Cell **37**:359–365.
9. **Brown, D. D., and M. S. Schlissel.** 1985. A positive transcription factor controls the differential expression of two 5S RNA genes. Cell **42**:759–767.
10. **Brown, R. S., C. Sander, and S. Argos.** 1985. The primary structure of transcription factor TFIIIA has 12 consecutive repeats. FEBS Lett. **186**:271–274.
11. **Drew, H. R.** 1984. Structural specificities of five commonly used DNA nucleases. J. Mol. Biol. **176**:535–557.
12. **Engelke, D. R., S.-Y. Ng, B. S. Shastry, and R. G. Roeder.** 1980. Specific interaction of a purified transcription factor with an internal control region of 5S RNA genes. Cell **19**:717–728.
13. **Fairall, L., D. Rhodes, and A. Klug.** 1986. Mapping of the sites of protection on a 5S RNA gene by the Xenopus transcription factor TFIIIA. A model for the interaction. J. Mol. Biol. **192**: 577–591.
14. **Galas, D., and A. Schmitz.** 1978. DNase footprinting: a simple method for the detection of protein-DNA binding specificity. Nucleic Acids Res. **5**:3157–3170.
15. **Giguere, V., S. M. Hollenberg, R. G. Rosenfeld, and R. M. Evans.** 1986. Functional domains of the human glucocorticoid receptor. Cell **46**:645–652.
16. **Ginsberg, A. M., B. O. King, and R. G. Roeder.** 1984. Xenopus 5S gene transcription factor, TFIIIA: characterization of a cDNA clone and measurement of RNA levels throughout development. Cell **39**:479–489.
17. **Green, S., and P. Chambon.** 1987. Oestradiol induction of a glucocorticoid response gene by a chimaeric receptor. Nature (London) **325**:75–78.
18. **Grunstein, M., and D. Hogness.** 1975. Colony hybridization: a method for the isolation of cloned DNAs that contain a specific gene. Proc. Natl. Acad. Sci. USA **72**:3961–3965.
19. **Hanas, J. S., D. J. Hazuda, D. F. Bogenhagen, F. H.-Y. Wu, and C.-W. Wu.** 1983. Xenopus transcription factor A requires zinc for binding to the 5S RNA gene. J. Biol. Chem. **258**:14120–14125.
20. **Hope, I. A., and K. Struhl.** 1985. GCN4 protein, synthesized in vitro, binds HIS3 regulatory sequences: implications for general control of amino acid biosynthetic genes in yeast. Cell **43**:177–188.
21. **Krieg, P. A., and P. A. Melton.** 1984. Functional messenger RNAs are produced by SP6 in vitro transcription of cloned DNAs. Nucleic Acids Res. **12**:7057–7070.
22. **Lassar, A. B., P. L. Martin, and R. G. Roeder.** 1983. Transcription of class III genes: formation of preinitiation complexes. Science **222**:740–748.
23. **Losa, R., and D. D. Brown.** 1987. A bacteriophage RNA polymerase transcribes in vitro through a nucleosome core without displacing it. Cell **50**:801–808.
24. **Lutter, L. C.** 1978. Kinetic analysis of deoxyribonuclease I cleavages in the nucleosome core: evidence for a DNA superhelix. J. Mol. Biol. **124**:391–420.
25. **Maniatis, T., S. Goodbourn, and J. A. Fischer.** 1987. Regulation

of inducible and tissue-specific gene expression. Science **236:** 1237–1245.
26. **Maxam, A. M., and W. Gilbert.** 1977. A new method for sequencing DNA. Proc. Natl. Acad. Sci. USA **74:**560–564.
27. **McConkey, G. A., and D. F. Bogenhagen.** 1987. Transition mutations within the *Xenopus borealis* somatic 5S RNA gene can have independent effects on transcription and TFIIIA binding. Mol. Cell Biol. **7:**486–494.
28. **McKnight, S. L., and R. Tjian.** 1986. Transcriptional selectivity of viral genes in mammalian cells. Cell **46:**795–805.
29. **Melton, D. A., P. A. Krieg, M. R. Rebagliati, T. Maniatis, K. Zinn, and M. R. Green.** 1984. Efficient in vitro synthesis of biologically active RNA and RNA hybridization probes from plasmids containing a bacteriophage SP6 promoter. Nucleic Acids Res. **12:**7035–7056.
30. **Miller, J., A. D. McLachlan, and A. Klug.** 1985. Repetitive zinc-binding domains in the protein transcription factor IIIA from Xenopus oocytes. EMBO J. **4:**1609–1614.
31. **Pelham, H. R. B., and D. D. Brown.** 1980. A specific transcription factor that can bind either the 5S RNA gene or 5S RNA. Proc. Natl. Acad. Sci. USA **77:**4170–4174.
32. **Pieler, T., B. Appel, S. L. Oei, H. Mentzel, and V. A. Erdmann.** 1985. Point mutational analysis of the Xenopus laevis 5S gene promoter. EMBO J. **4:**1847–1853.
33. **Pieler, T., J. Hamm, and R. G. Roeder.** 1987. The 5S gene internal control region is composed of three distinct sequence elements, organized as two functional domains with variable spacing. Cell **48:**91–100.
34. **Rhodes, D., and A. Klug.** 1986. An underlying repeat in some transcriptional control regions corresponding to half a double helical turn of DNA. Cell **46:**123–132.
35. **Rusconi, S., and K. R. Yamamoto.** 1987. Functional dissection of the hormone and DNA binding activities of the glucocorticoid receptor. EMBO J. **6:**1309–1315.
36. **Ryrie, I. J., and A. Galagher.** 1979. The yeast mitochondrial ATPase complex. Subunit composition and evidence for a latent protease contaminant. Biochim. Biophys. Acta **545:**1–14.
37. **Sakonju, S., D. F. Bogenhagen, and D. D. Brown.** 1980. A control region in the center of the 5S RNA gene directs specific initiation of transcription. I. The 5′ border of the region. Cell **19:**13–25.
38. **Sakonju, S., and D. D. Brown.** 1982. Contact points between a positive transcription factor and the Xenopus 5S RNA gene. Cell **31:**395–405.
39. **Sakonju, S., D. D. Brown, D. Engelke, S.-Y. Ng, B. S. Shastry, and R. G. Roeder.** 1981. The binding of a transcription factor to deletion mutants of a 5S ribosomal RNA gene. Cell **23:**665–669.
40. **Schuh, R., W. Aicher, G. Ulrike, S. Cote, A. Preiss, D. Maier, E. Seifert, U. Nauber, C. Schroder, R. Kemler, and H. Jackle.** 1986. A conserved family of nuclear proteins containing structural elements of the finger protein encoded by Kruppel, a Drosophila segmentation gene. Cell **47:**1025–1032.
41. **Segall, J., T. Matsui, and R. G. Roeder.** 1980. Multiple factors are required for the accurate transcription of purified genes by RNA polymerase III. J. Biol. Chem. **255:**11986–11991.
42. **Smith, D. R., I. J. Jackson, and D. D. Brown.** 1984. Domains of the positive transcription factor specific for the Xenopus 5S RNA gene. Cell **37:**645–652.
43. **Taylor, W., I. J. Jackson, N. Siegel, A. Kumar, and D. D. Brown.** 1986. The developmental expression of the gene for TFIIIA in Xenopus laevis. Nucleic Acids Res. **14:**6185–6195.
44. **Tso, J. Y., D. J. Van Den Berg, and L. J. Korn.** 1986. Structure of the gene for Xenopus transcription factor TFIIIA. Nucleic Acids Res. **14:**2187–2200.
45. **Tullius, T. D., and B. A. Dombroski.** 1986. Hydroxyl radical "footprinting": high resolution information about DNA-protein contacts and application to lambda repressor and cro protein. Proc. Natl. Acad. Sci. USA **83:**5469–5473.
46. **Tullius, T. D., B. A. Dombroski, M. E. A. Churchill, and L. Kam.** 1987. Hydroxyl radical footprinting: a high-resolution method for mapping protein-DNA contacts. Methods Enzymol. **155:**537–558.
47. **Wolffe, A. P., E. Jordan, and D. D. Brown.** 1986. A bacteriophage RNA polymerase transcribes through a Xenopus 5S RNA gene transcription complex without disrupting it. Cell **14:**381–389.